Published in final edited form as:
J Am Soc Mass Spectrom. 2008 June ; 19(6): 780–789. doi:10.1016/j.jasms.2008.01.001.

Probing the Gas Phase Folding Kinetics of Peptide Ions by IR Activated DR-ECD

Cheng Lin[a], **Jason J. Cournoyer**[a,b], and **Peter B. O'Connor**[a]

[a] Mass Spectrometry Resource, Department of Biochemistry, Boston University School of Medicine, Boston, MA 02118, USA

[b] Department of Chemistry, Boston University, Boston, MA 02215, USA

Abstract

The effect of infrared (IR) irradiation on the electron capture dissociation (ECD) fragmentation pattern of peptide ions was investigated. IR heating increases the internal energy of the precursor ion, which often amplifies secondary fragmentation, resulting in the formation of w-type ions as well as other secondary fragments. Improved sequence coverage was observed with IR irradiation before ECD, likely due to the increased conformational heterogeneity upon IR heating, rather than faster breakdown of the initially formed product ion complex, as IR heating after ECD did not have similar effect. Although the ECD fragment ion yield of peptide ions does not typically increase with IR heating, in double resonance (DR) ECD experiments, fragment ion yield may be reduced by fast resonant ejection of the charge reduced molecular species, and becomes dependent on the folding state of the precursor ion. In this work, the fragment ion yield was monitored as a function of the delay between IR irradiation and the DR-ECD event to study the gas phase folding kinetics of the peptide ions. Furthermore, the degree of intra-complex hydrogen transfer of the ECD fragment ion pair was used to probe the folding state of the precursor ion. Both methods gave similar refolding time constants of ~1.5 s^{-1}, revealing that gaseous peptide ions often refold in less than a second, much faster than their protein counterparts. It was also found from the IR-DR-ECD study that the intra-molecular $H^{\bullet}$ transfer rate can be an order of magnitude higher than that of the separation of the long-lived c/z product ion complexes, explaining the common observation of $c^{\bullet}$ and z type ions in ECD experiments.

Introduction

One of the major challenges of modern structural biology is to understand the process of *in vivo* folding of a protein into a well-defined, biologically active structure [1, 2]. The effects of aqueous solvation and the intrinsic intramolecular interactions may be better revealed by studying the protein conformation in the gas phase in the absence of solvents. Making use of the soft ionization method of electrospray ionization (ESI) [3], a number of mass spectrometry (MS) based methods have been applied to investigate the protein conformation in the gas phase, including the ESI charge state distribution to determine the availability of ionization basic sites [4, 5], H/D exchange (HDX) to identify the exposed region of the

Address reprint requests to Dr. Peter O'Connor, Department of Biochemistry, Boston University School of Medicine, Boston, MA 02118, USA. poconnor@bu.edu.

conformation [6–10], drift tube ion mobility spectrometry (IMS) to measure the conformational cross section [10–13], high-field asymmetric waveform ion mobility spectrometry (FAIMS) to separate different conformers [10, 14, 15], infrared photodissociation spectroscopy (IRPDS) to probe the hydrogen bonding [16–20], and electron capture dissociation (ECD) [21, 22] to locate the noncovalent tertiary bonding [23–26]. Particularly, ECD based methods have been used to study the gas phase unfolding and refolding kinetics of protein ions [24, 25].

ECD in Fourier-transform ion cyclotron resonance mass spectrometry (FT-ICR-MS or FTMS) [27, 28] has quickly found wide application in both top-down and bottom-up proteomics [21, 29–33], as well as in identifying and locating post-translational modifications (PTMs) [34–38]. As a non-threshold dissociation method, the ECD fragment ion yield of a protein ion is not only affected by its sequence, but also by its higher order structures [15, 21, 26, 39, 40]. This is the basis of studying protein conformation and folding process by ECD. Noncovalent intramolecular interactions of protein ions may prevent fragment ion separation, leading to decreased product ion yield and poor sequence coverage, both of which can be improved in activated ion (AI)-ECD, where protein ions are unfolded [41–45]. Ion activation is typically done by collisions with background gas molecules [41, 43, 45], raising the ambient temperature [16, 45], or infrared (IR) laser irradiation [42, 44–46]. Efficient energy transfer via multiple collisions with gas molecules requires the cell pressure to be increased to the 10^{-6} Torr range, which in turn requires a long pump-down time (~10 seconds typically) before the pressure is suitable for trapped ion excitation and detection with a sufficiently long transient for good resolving power, making it unattractive for high-throughput analysis or signal averaging when the sample comes in limited amount. Moreover, collisional activation via sustained off-resonance irradiation (SORI) [47, 48] of precursor ions is complicated by tuning of optimal conditions for each individual ion, while “in-beam” activation (as in in-beam ECD [41] or plasma ECD experiments [43]) has the limitation of not being able to isolate the precursor ions. Raising the temperature to and keeping it at a well defined value in the ICR cell is not always possible with every FT-ICR mass spectrometer [49, 50]. Even when it is possible, it is still inconvenient in that it takes time to heat up the cell before AI-ECD experiments and to cool the cell back down for normal operation afterwards. Furthermore, heating also usually results in an undesirable increase in cell pressure. IR irradiation, on the other hand, is fast, easy to implement, allows precursor ion isolation, and does not result in cell pressure increase, making it the preferred method for ion activation in AI-ECD experiments.

Simultaneous introduction of IR laser and electron beam to intersect the ion cloud in the center of the ICR cell has been previously done by either bringing in one beam off-axis while keeping the other on-axis [42, 45], or introducing the IR beam through a hollow electron gun mounted on-axis and letting the ring-shaped electron beam be compressed by the magnetic field gradient [44]. It has been shown extensively that ion activation by IR laser absorption lead to enhanced fragmentation in protein ion ECD. The heated, unfolded protein ion can also cool and refold in the gas phase, and ECD fragment ion yield with ECD conducted at various delays after the IR irradiation should provide a measure of the extent of protein refolding [25].

It should be noted that the increased product ion formation results from the breakdown of the initially formed long-lived fragment ion complexes that stay unseparated during the excitation/detection event in absence of ion activation. Unlike larger protein ions, intramolecular noncovalent interactions in peptide ions are not as numerous. Thus, the resulting fragment ion complexes in ECD are often short lived, and easily separate to generate individual product ions before ion detection. Consequently, little enhancement in fragment ion yields were expected in AI-ECD of smaller peptide ions. Nonetheless, the

existence of these ion complexes in peptide ECD is evident, as suggested by a number of experiments. Deuterium scrambling in ECD of a selectively deuterated linear peptide was readily present, most likely due to intermolecular H/D exchange in the fragment ion complexes [51]. Formation of radical $c^{\bullet}$ ions and even-electron *z* ions is often observed in peptide ECD experiments, postulated to be the result of H-atom abstraction from the *c*-ion backbone or side chains by the α-carbon radical on the $z^{\bullet}$ ion [51–53]. This hypothesis correlates well with the observation of the decreased $c^{\bullet}/c$ ratio and the increased $z^{\bullet}/z$ ratio upon ion activation [53], when *c*/*z* ion separation rate is comparable to that of the H-atom transfer. The knowledge that the $c^{\bullet}/c$ ratio decreases and the $z^{\bullet}/z$ ratio increases upon ion activation has been utilized to distinguish the type of ions formed in ECD [53]. Finally, in double resonance (DR)-ECD experiments, resonant ejection of the charge reduced species and the isobaric fragment ion complexes resulted in abundance decreases of many ECD fragments from peptide ions, thus directly showing that formation of these ECD fragment ions proceeds via radical complex intermediates that have a lifetime at least comparable to that of the ejection time, typically in milliseconds [54].

Experimental

Experiments were carried out on a custom-built qQq-FT-ICR mass spectrometer with an external electrospray ionization source [55, 56]. All peptide were purchased from Sigma Aldrich (St. Louis, MO), and used without further purification. The samples were diluted to ~5 pmol/μL in 50:50:1 H_2O:CH_3OH:HCOOH solution, and electrosprayed from glass capillary nanospray tips to generate multiply charged ions. Ions of interest were isolated and accumulated in the front end quadrupoles before entering the cell, where they were subjected to ~100 ms low energy electron irradiation from an on-axis indirectly heated dispenser cathode (model STD200, Heatwave, Watsonville, CA). In double resonance experiments, the charge reduced molecular ions were resonantly ejected from the cell by applying a single frequency excitation waveform with a peak-to-peak amplitude of 2.5 to 40 Volts during the electron irradiation period.

IR light (10.6 μm) from a CO_2 laser (Synrad, Mukilteo, WA) was introduced into the ICR cell through a BaF_2 window, ~ 0.87 inch off center. The IR laser beam traveled parallel to the magnetic field axis towards a mirror mounted on the cell end trapping plate, with the mirror tilted at ~4.2° such that the reflected beam passed through the center of the cell. For initial alignment, a photodiode was installed on the other cell trapping plate, located diagonally from the mirror, also ~ 0.87 inch off center. Overlap of the reflected beam from an alignment diode laser (590 nm) mounted just outside of the laser exit and the photodiode was optimized by maximizing the photoconductivity of the photodiode. The laser beam path was then constructed and defined by insertion and locking of two irises around the beam, and the photodiode was removed as it was not UHV compatible. Final alignment was achieved by maximizing the fragmentation of ubiquitin ions by the 10.6 μm laser. With the IR beam intersecting the ion cloud at an angle, higher fragmentation yield may be achieved by increasing the trapping voltage to squeeze ion cloud axially. However, such was not implemented in IR-DR-ECD experiments, as the objective was merely to heat up the ions gently rather than to achieve maximum fragmentation. The IR irradiation time was adjusted to achieve maximum ion activation without fragmentation.

A typical spectrum was the sum of 10 scans, acquired at 1 MHz sampling rate and with 512 k point buffer size, corresponding to a 0.524 second transient. The digitized transients were zero-filled twice and fast Fourier transformed without apodization to produce the magnitude mode mass spectra. Because all fragment ions were singly charged, their abundances were calculated directly from peak heights without the need of charge correction to account for ICR response. With the theoretical Fourier-transform limit mass resolving power (*f***t*/*2*)

being a mere 28,134 at *m/z* ~1000, it was not possible to separate the A+1 isotopic peak of $c^{\bullet}$ or $z^{\bullet}$ ions from the monoisotopic peak of the corresponding c or z ions. Thus, when interference existed, the theoretical A+1 contribution from the odd-electron species was subtracted to give the correct ion abundance of the monoisotopic even-electron species.

Results and Discussion

Effects of IR Heating on ECD Pattern of Substance P

As a first example to show the effects of IR heating on ECD pattern of peptide ions, the ECD spectra of substance P (RPKPQQFFGLM-NH_2) both without (Figure 1a) and with IR heating (200 ms duration) before (Figure 1b) and after (Figure 1c) electron irradiation were acquired. Since both basic residues are located near the N-terminus, it is of no surprise that ECD of substance P produced mostly *c*-type ions, with the only *z*-type ion being the z_9 that contains the lysine residue. The c_2 ion is not present in the spectrum, even though its *m/z* (273.2) is well above the Nyquist frequency limit used (corresponding to *m/z* ~215). Post-heating the ion cloud with 200 ms IR irradiation did not change the ECD pattern significantly, with the c_2 ion still missing from the spectrum (Figure 1c). Therefore, the absence of c_2 cannot solely be the result of intra-complex noncovalent bonding holding the fragment ion pair together. It has been reported that at 86 K, ECD of substance P generated only two *c* ions (c_7 and c_{10}), which was proposed to be the result of reduced conformational heterogeneity at lower temperature [57]. The calculated low-energy gas-phase structures of doubly charged substance P involve solvation of the protonated Lys3 away from the N-terminus [58]; thus, even at room temperature, the formation of c_2 is disfavored. The addition of a third charge by either adding a proton or replacing a proton with a divalent metal ion significantly changed the gas phase conformation of substance P, particularly the solvation of the Lys3 proton, as evidenced by the abundant c_2 ion formation [59]. In accordance with these results, preheating the precursor ions with IR also led to the formation of c_2 (Figure 1b), likely due to the increased internal energy of the precursor ions by IR heating allowing the protonated Lys3 to be solvated near the N-terminus. The conformational change also led to the disappearance of the z_9 ion, as c_2 formation requires the protonated Lys3 side chain to be hydrogen bonded to the Pro2 carbonyl and neutralized during electron capture, preventing the Arg1 side chain from binding there, which was necessary for z_9 formation. The disappearance of z_9 ions with IR heating may also be the result of secondary fragmentation, although this is unlikely because neither smaller z_n ions nor internal fragment ions were observed. Since the conformational change had to take place before ECD to direct the formation of product ions/neutrals, post-heating the ions would not have similar effects.

In addition to the commonly formed *c* and $z^{\bullet}$ type ions, ECD of substance P also produced some $c^{\bullet}$ type ions ($c_4^{\bullet}$ and $c_5^{\bullet}$ as shown in the insets of Figure 1), which disappeared completely when the precursor ions were heated with IR irradiation before ECD. It is generally believed that ECD produces *c* and $z^{\bullet}$ type ions first and the formation of $c^{\bullet}$ and *z* ions is the result of intra-complex hydrogen radical transfer, the extent of which depends on the stability of the $z^{\bullet}$ radical as well as the lifetime of the initially formed $c/z^{\bullet}$ ion pair [51, 52, 54]. IR heating before ECD can disrupt the intramolecular interactions that hold the $c/z^{\bullet}$ ion pair together, leading to shortened lifetime and less $c^{\bullet}$ and *z* ion formation. On the other hand, post-ECD IR heating appeared to have very little effect, presumably because the intra-molecular H transfer is a fast process that completed before the ion pair complex was heated sufficiently for dissociation. It is also interesting to note that c_4 and c_5 were the only two N-terminal fragment ions showing a significant drop in ion abundances in the DR-ECD experiment (Supplemental Figure 1), further suggesting that $c^{\bullet}$ ion formation requires a long-lived ion pair complex. Although the abundances of $c_4^{\bullet}$ and $c_5^{\bullet}$ dropped significantly in DR-ECD, a substantial amount of $c^{\bullet}$ ions remained. Thus, the intra-complex hydrogen

radical transfer must have taken place on a timescale at least comparable to that of ion ejection, i.e. in sub-milliseconds.

Enhanced Fragment Ion Yield in IR-ECD

While fragment ion yield enhancement and improved sequence coverage in AI-ECD of protein ions were largely attributed to the breaking of noncovalent interactions to facilitate the fragment ion separation and detection, it is clear from the previous example that increased conformational heterogeneity may also play an important role. In IR-ECD of substance P, this resulted in c_2 ion formation and z_9 disappearance with no other significant change in the ECD pattern. A more drastic change in the ECD pattern with IR heating was observed in IR-ECD of fibrinopeptide B (EGVNDNEEGFFSAR), as shown in Figure 2. ECD of fibrinopeptide B generates mostly *z* type ions due to charge retention on the C-terminal arginine side chain upon electron capture, with a small peak corresponding to the c_{13} ion (upper spectrum, Figure 2a). $z_2^{\bullet}$ (*m/z* ~230) was missing from the spectrum, and $z_3^{\bullet}$ was barely observable. 150 ms IR irradiation before ECD (upper spectrum, Figure 2b) led to formation of the z_2 ion, and a large abundance increase for many small *z* ions (z_3 to z_6) as well as c_{11} and c_{13} ions. In the DR-ECD experiment, *z*-ions up to z_8 showed appreciable abundance drop upon resonant ejection of the charge reduced molecular ion (at *m/z* ~1571) during the ECD event (upper spectrum, Figure 2a), suggesting that the C-terminal arginine side chain was hydrogen bonded to the side chains of Asn4 to Glu8 at room temperature, which is highly likely since this sequence contains three acidic residues. The folded structure may also sterically restrict the access of the N-terminal $-NH_3^+$ group (or other charge sites) to the carbonyls of Gly9 through Ala13, thus minimizing ECD near this region. Such steric restriction would be removed and the conformation heterogeneity increased when the peptide was unfolded by IR heating prior to electron irradiation, resulting in the fragment ion yield increase as observed. In order to open up new fragmentation channels, the unfolding and the conformational change have to take place before the dissociation event. IR irradiation after ECD did not change the ECD pattern significantly (spectrum not shown). Once again, it shows that the increased fragment ion yield in AI-ECD of small peptide ions is more likely to be the result of conformational change than the ease of fragment ion separation.

Secondary Fragment Ion Formation in IR-ECD of Fibrinopeptide B

ECD of a multiply charged peptide ion produces an even-electron fragment (*c*-ion) and an odd-electron fragment ($z^{\bullet}$ ion). The radical site on the odd-electron fragment can initiate further reactions such as intra-complex hydrogen radical transfer which leads to the formation of $c^{\bullet}$ and *z* ions [52], or secondary fragmentation with little or no activation barrier [22, 60–63]. Secondary side chain fragmentation leading to the formation of *d*- and *w*- type ions is well documented in the ECD literature, and has found application in *de novo* sequencing for its ability to distinguish between Leu and Ile residues [44, 60, 64, 65]. Abundant *w* ion formation was apparent in the IR-ECD experiment (Figure 2b), in accord with previous observations in hot ECD and AI-ECD, where extra energy seem to enhance the *w* ion formation. Many other secondary fragment ions (peaks marked with # in Figure 2b) were also present in the IR-ECD spectrum, corresponding mostly to side chain losses from the z-ions. It is important to heat up the precursor ion before ECD, instead of the fragment ions after ECD, as post-ECD IR irradiation generates little secondary fragment ions. This might be due to rapid radical stabilization [66–68] via radical rearrangement, such as intra-complex H transfer, proline ring opening, or radical trapping near the aromatic group, before IR heating. Secondary backbone fragmentations dominated the ECD spectra of cyclic peptides [22], but no internal fragment ions were found in the IR-ECD spectrum of fibrinopeptide B, presumably because of the charge locations at the termini.

Unfolding and Refolding of Peptide Ion by IR Irradiation

AI-ECD has been used to study protein folding in the gas phase, by monitoring the fragment ion yield, which often increases with ion activation, due to breaking of intra-molecular hydrogen bonds that prevent fragment ion separation [24, 25]. The challenge of extending this method to peptide folding studies is that the lifetime of the fragment ion complexes from peptide ion ECD is often much shorter than the delay between the ECD event and ion excitation/detection, and as the result, nearly all fragment ions are readily detected, with or without ion activation. This difficulty may be circumvented by applying the DR-ECD method, where resonant ejection of the fragment ion complexes during ECD can reduce the fragment ion abundance [54]. Because of the rapid ejection time, even fragment ions from intermediates of millisecond lifetime, as is typical in peptide ion ECD, can experience significant abundance drop in DR-ECD, and the subsequent increase when IR irradiation is applied to unfold the precursor ions.

A greater abundance drop in DR-ECD indicates a longer lifetime of the intermediate through which the product ions are formed, as the result of a more folded structure of the precursor ion. Compared to the sharp abundance drop in DR-ECD of room temperature fibrinopeptide B (upper spectrum, Figure 2a), many small *z* ions experienced only moderate to little drop in abundance with pre-ECD IR irradiation (lower spectrum, Figure 2b), suggesting that most of the intramolecular hydrogen bonds were already broken. The lifetime of the intermediate can be calculated by assuming that separation of a fragment ion pair follows first-order unimolecular dissociation kinetics [54]. Figure 3 plots the abundance of the intact c_7/z_7 pair, which is calculated as the difference between the abundance of z_7 ion in normal ECD and that in DR-ECD, against the ejection time with DR-ECD taking place at various time delays after the IR irradiation (or without IR irradiation). The single exponential decay fit gives the lifetime of the c_7/z_7 ion pair complex of ~2.6 ms without pre-ECD IR heating, and ~0.7 ms when ECD was performed immediately after the IR irradiation. When there was a delay between the IR and the DR-ECD event (Figure 2c), the lifetime of the intermediate increased to ~1.1 ms with a 100 ms delay, and ~1.9 ms with a 800 ms delay. Clearly, the unfolded peptide ion can cool and refold back to a more compact structure, particularly in absence of solvent molecules in the gas phase. The refolding process took place in several hundred milliseconds to a few seconds, but a more quantitative assessment of the refolding time constant would require a properly constructed kinetic model.

Refolding Kinetics of Fibrinopeptide B Probed by the Fragment Ion Yield in DR-ECD

A simple two-state model was used to study the refolding kinetics, which assumes that a peptide ion can only exist in one of the two states: a folded state, or an unfolded state. All *c/z* ion pairs from an unfolded peptide ion will break before ejection, but only a fraction (*x*) of these ion complexes from a folded peptide ion will break before ejection. The value of *x* depends on both the amplitude of the resonant ejection waveform and the lifetime of the intermediate, and it can be obtained from the DR-ECD experiment without IR heating, assuming that all peptide ions are folded to start with. If DR-ECD is performed at a delay of *t* after the IR irradiation, then the ratio (*r*) of the fragment ion abundance with resonant ejection to the one without resonant ejection can be expressed as:

$$r = y + (1 - y) * x \quad [1]$$

where *y* is the fraction of the peptide ions remaining unfolded at time delay *t*. This ratio (*r*) should drop as the delay *t* increases and the peptide ions refold. Since *r* can be obtained experimentally, and *x* is just *r* without IR irradiation, the fraction of the unfolded peptide ions, *y*, at any given delay after the IR irradiation can be calculated according to equation 1.

Assuming first order refolding kinetics, one can obtain the refolding time constant k_{refold} by fitting y as a function of t to a single exponential decay. Figure 4 shows one such plot using the z_7 yield in DR-ECD with 20 V_{pp} ejection voltage as the probe for precursor ion folding state. Abundances from both the odd and even electron z_7 ions are included, because the formation of either results from the breaking of the same initially formed $c_7/z_7^{\bullet}$ complex. The best fit gives a k_{refold} of 1.55 ± 0.10 s^{-1}, corresponding to a half-life of 0.45 s, which correlates well with Figure 2c. This is much faster than that for protein ions, which typically take minutes to refold in the gas phase [24]. Presumably, the reduced dimension of the potential energy surface of the smaller peptide ion makes it faster to find its low energy structures than its protein counterparts.

Refolding Kinetics of Fibrinopeptide B Probed by the Intra-Complex Hydrogen Transfer

The key to the study of gas phase peptide folding by AI-ECD is to find a suitable property that varies with folding states, such as the fragment ion yield in DR-ECD experiment (*vide infra*). Figure 5a shows that even though the total abundance of the z_7 ions in ECD did not change much with the IR heating, the ratio of z to $z^{\bullet}$ ion abundance increased as the delay between IR and ECD increased. This should come as no surprise, as even-electron z ions are the products of intra-complex hydrogen radical transfer, which should decrease as the IR heating unfolds the peptide, leaving the product ion complex too short-lived to complete the $H^{\bullet}$ transfer. The same two-state model can be used to study the peptide ion refolding, with a slightly different definition for folding and unfolding states. An unfolded peptide should only produce $z^{\bullet}$ ions, as there is nothing to hold the fragment ion pair together for $H^{\bullet}$ transfer to take place. If a peptide is folded, however, a fraction (x) of the $z^{\bullet}$ ions can abstract a hydrogen atom to form z ions, and the value of x can be obtained from the ECD experiment without IR heating, assuming all peptide ions are unfolded before IR irradiation. If y is the fraction of peptide ions remaining unfolded at a delay of t after IR, we have:

$$\frac{[z]_t}{[z]_r+[z^{\bullet}]_t}=(1-y)*x \qquad [2]$$

Since the fraction of the even-electron z ions in the total z ion population can be directly measured in the ECD spectrum, y can be calculated for any given delay t. Once again, plotting y as a function of t should give a single exponential decay if the refolding process follows first order kinetics. Figure 5b plots the percentage of the unfolded peptide ions against delay t, using the $[z_7]/([z_7]+[z_7^{\bullet}])$ to calculate y. The best fit gives k_{refold} of 1.52 ± 0.14 s^{-1}, corresponding to a 0.45 s refolding time, nearly the same as that obtained in the IR-DR-ECD approach.

Furthermore, it is also possible to estimate the intra-complex H-transfer rate based on the abundance ratio of the even and odd-electron fragment ions and the fragment ion pair separation rate measured in the DR-ECD experiments. Scheme 1 illustrates the formation of $c^{\bullet}$ and z ions as the result of intra-complex H-transfer:

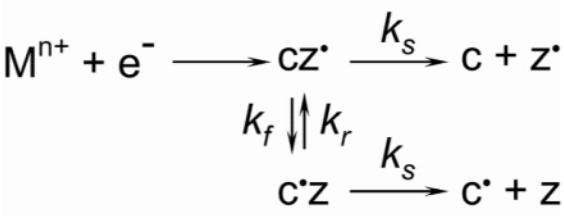

The rate equations for relevant species in scheme 1 are shown in equations 3:

$$\begin{aligned}\frac{d[cz^\bullet]}{dt} &= -k_s[cz^\bullet] - k_f[cz^\bullet] + k_r[c^\bullet z] \\ \frac{d[c^\bullet z]}{dt} &= -k_s[c^\bullet z] + k_f[cz^\bullet] - k_r[c^\bullet z] \\ \frac{d[z^\bullet]}{dt} &= k_s[cz^\bullet] \\ \frac{d[z]}{dt} &= k_s[c^\bullet z]\end{aligned} \quad [3]$$

Equation set 3 can be solved analytically, giving:

$$\begin{aligned}[cz^\bullet]_t &= \frac{[cz^\bullet]_0}{k_f+k_r}\left[k_r e^{-k_s t} + k_f e^{-(k_f+k_r+k_s)t}\right] \\ [c^\bullet z]_t &= \frac{[cz^\bullet]_0}{k_f+k_r}\left[k_f e^{-k_s t} - k_f e^{-(k_f+k_r+k_s)t}\right] \\ [z^\bullet]_t &= \frac{[cz^\bullet]_0}{k_f+k_r}\left\{k_r\left[1-e^{-k_s t}\right] + \frac{k_s k_f}{k_f+k_r+k_s}\left[1-e^{-(k_f+k_r+k_s)t}\right]\right\} \\ [z]_t &= \frac{[cz^\bullet]_0}{k_f+k_r}\left\{k_f\left[1-e^{-k_s t}\right] - \frac{k_s k_f}{k_f+k_r+k_s}\left[1-e^{-(k_f+k_r+k_s)t}\right]\right\}\end{aligned} \quad [4]$$

As stated earlier, for most peptide ECD experiments, when the excite/detect event happens, nearly all fragment ion pairs have already fallen apart. In other words, t in the above solution at the time of detection can be approximated as infinity when considering the product branching ratio, giving:

$$\frac{[z^\bullet]}{[z]} = \frac{k_r+k_s}{k_f} \quad [5]$$

In the extreme case where the separation of product ions is much slower than the intra-complex hydrogen transfer, i.e., $k_s \ll k_r$, the ratio is governed primarily by thermodynamics, giving the equilibrium constant between the $c/z^\bullet$ and $c^\bullet/z$ ion pairs. In the other extreme case where the separation of product ions is much faster than the intra-complex hydrogen transfer, i.e., $k_s \gg k_r$, the ratio is kinetically controlled, with the equation 5 reduced to the familiar form of $[z^\bullet]/[z] = k_s / k_f$, giving the branching ratio of a parallel or competitive reactions.

Equation 5 can be rearranged as:

$$\frac{[z^\bullet]}{[z]} = \frac{k_r}{k_f} + \frac{1}{k_f}k_s \quad [6]$$

With different delays between IR and ECD events, a set of $[z^\bullet]/[z]$ values can be obtained, with the corresponding k_s calculated from the DR-ECD experiment, and fit into a straight line. Figure 6 shows one such plot for fibrinopeptide B, using the ratio of $[z_7^\bullet]/[z_7]$ and the k_s values from figure 3. The linear regression fit gives a k_f of 2.0 ms^{-1} and a k_r of 2.4 ms^{-1}. The quality of the fit is only moderate, with a ~0.94 correlation coefficient, likely because of the assumption that k_f and k_r are independent of the folding state. Nevertheless, the obtained hydrogen transfer rates are nearly an order of magnitude higher than the rate of product ion pair separation under normal ECD conditions. It is thus of no surprise that $c^\bullet$ and z type ions are commonly observed in peptide ion ECD, as the initially formed $c/z^\bullet$ ion pairs have plenty of time to undergo intra-complex hydrogen transfer before they separate to produce individual fragment ions. Despite this fast intra-complex hydrogen transfer rate, $c^\bullet$ and z type ions are rarely observed in protein ion ECD experiments. Columbic repulsion between

positively charged *c* and $z^{\bullet}$ counterparts, which are not present in the ECD products of doubly charged tryptic peptide ions, may lead to faster product ion separation in protein ion ECD, contributing to this lack of H-transfer products. However, such is not always the case as demonstrated in the DR-ECD experiment of bovine ubiquitin, where many product ions displayed significant abundance drop upon resonant ejection of the charge reduced molecular ion, indicating millisecond lifetimes (at least) of the fragment ion complexes [54]. Presumably, the much more extensive noncovalent interactions in protein ions outweigh the columbic repulsion in determining the lifetime of intermediates. Most likely, in protein ion ECD, H-transfer still occurs extensively before product ion separation, but somehow preferentially within the $z^{\bullet}$ fragment itself leading to radical stabilization, possibly due to the tertiary structure of the gas phase protein ion.

The percentage of the unfolded peptide ions at any given time delay *t* is very different for figure 4 and figure 5, because of different definitions of an unfolded peptide in two methods. For the DR-ECD approach, fragment ion pair complexes from an unfolded peptide cannot have a lifetime longer than the ejection time, while for the H-transfer method, they cannot undergo any (observable) intra-complex H-transfer before they break apart to produce *c* and $z^{\bullet}$ ions. Since $t_{1/2}$ of H-transfer is much shorter than the ejection time applied in DR-ECD studies, a significant amount of ion complexes from “unfolded” peptide ions in the DR-ECD approach may still live long enough to generate H-transfer products, and are therefore considered “folded” peptides in the H-transfer method. Regardless, despite different ways to probe the folding state of the peptide ions, these two methods give similar refolding time constants. When there are abundant $c^{\bullet}$ or *z* type ions, the H-transfer approach is convenient, and has the potential of probing folded state that produces fragment ion pairs shorter lived than that can be probed by the IR-DR-ECD approach, as the typical half-life for H-transfer is only a fraction of the ejection time commonly applied. However, not all peptide ions produce appreciable amount of $c^{\bullet}$ or *z* type ions, and when this is the result of intra-fragment ion radical stabilization rather than ultra-fast fragment ion pair separation, the IR-DR-ECD method should provide an excellent way to study the folding kinetics.

Conclusions

The effect of IR irradiation on the ECD fragmentation pattern of peptide ions was investigated using two model peptides, substance P and fibrinopeptide B. The increased internal energy of the precursor ions often led to amplified secondary fragmentation in IR-ECD. Ion activation was accompanied by increased conformational heterogeneity and weakened non-covalent intra-molecular interactions. Improved sequence coverage was observed in both peptide ions, likely the result of the conformational change, rather than faster fragment ion separation, as suggested by the lack of sequence coverage improvement when IR irradiation was introduced after the ECD event. Weakening of non-covalent interactions did not lead to appreciable enhancement of fragment ion yield, because even at ambient temperature, fragment ion pair separation from small peptide ECD was nearly complete before ion excitation and detection, making IR-ECD unsuitable for probing gas phase peptide ion folding states. However, IR unfolding of peptide ions did lead to increased $c/c^{\bullet}$ and decreased $z/z^{\bullet}$ ratios, which can be utilized to study the peptide refolding process. The refolding rate constant for fibrinopeptide B was measured to be ~1.5 s^{-1}, much faster than that of protein ions. Linear regression fit based on a simplified kinetic model of intra-complex hydrogen transfer gave the H-transfer rate constant of ~2 ms^{-1}, about an order of magnitude faster than the separation rate of the long-lived c/z ion pair, explaining the ubiquitous presence of $c^{\bullet}$ and *z* type ions in peptide ion ECD spectra. Alternatively, the folding kinetics of peptide ions can be studied by the IR-DR-ECD method. Rapid resonant ejection of the charge reduced species during ECD can lead to difference in fragment ion yields for folded and unfolded peptide ions, which were indistinguishable under normal

ECD conditions, thus making it a suitable probe for folding studies. This approach gave very similar folding time as that obtained by monitoring the extent of hydrogen transfer, and can be especially useful when no appreciable $c^{\bullet}$ and z type ions are present in the ECD spectrum.

Supplementary Material

Refer to Web version on PubMed Central for supplementary material.

Acknowledgments

The authors gratefully acknowledge the financial support from the National Institutes of Health (Grants NIH/NCRR P41RR10888, NIH/NHLBI N01HV28178, and NIH/NIGMS R01GM078293), MDS SCIEX, and the ACS Petroleum Research Fund. We thank Dr. Chunxiang Yao and Xiaojuan Li for helps with experiments.

References

1. Gething MJ, Sambrook J. Protein Folding in the Cell. Nature. 1992; 355:33–45. [PubMed: 1731198]
2. Dobson CM. Protein folding and misfolding. Nature. 2003; 426:884–890. [PubMed: 14685248]
3. Fenn JB, Mann M, Meng CK, Wong SF, Whitehouse CM. Electrospray ionization for mass spectrometry of large biomolecules. Science. 1989; 246:64–71. [PubMed: 2675315]
4. Chowdhury SK, Katta V, Chait BT. Differences in Charge States of Electrosprayed Native and Denatured Proteins. J Am Chem Soc. 1990; 112:9012.
5. Loo JA. Electrospray ionization mass spectrometry: a technology for studying noncovalent macromolecular complexes. Int J Mass Spectrom. 2000; 200:175–186.
6. Winger BE, Light-Wahl KJ, Rockwood AL, Smith RD. Probing Qualitative Conformation Differences of Multiply Protonated Gas-Phase Proteins via H/D Isotopic Exchange with D2O. J Am Chem Soc. 1992; 114:5897–5898.
7. Suckau D, Shi Y, Beu SC, Senko MW, Quinn JP, Wampler FM III, McLafferty FW. Co-Existing Stable Conformations of Gaseous Protein Ions. Proc Natl Acad Sci USA. 1993; 90:780.
8. Freitas MA, Hendrickson CL, Emmett MR, Marshall AG. Gas-phase bovine ubiquitin cation conformations resolved by gas-phase hydrogen/deuterium exchange rate and extent. Int J Mass Spectrom. 1999; 187:565–575.
9. Wyttenbach T, Bowers MT. Gas phase conformations of biological molecules: The hydrogen/deuterium exchange mechanism. J Am Soc Mass Spectrom. 1999; 10:9–14.
10. Robinson EW, Williams ER. Multidimensional separations of ubiquitin conformers in the gas phase: Relating ion cross sections to H/D exchange measurements. J Am Soc Mass Spectrom. 2005; 16:1427–1437. [PubMed: 16023362]
11. Clemmer DE, Hudgins RR, Jarrold MF. Naked Protein Conformations - Cytochrome-C in the Gas-Phase. J Am Chem Soc. 1995; 117:10141–10142.
12. Jarrold MF. Peptides and proteins in the vapor phase. Annu Rev Phys Chem. 2000; 51:179–207. [PubMed: 11031280]
13. Badman ER, Myung S, Clemmer DE. Evidence for unfolding and refolding of gas-phase cytochrome c ions in a Paul trap. J Am Soc Mass Spectrom. 2005; 16:1493–1497. [PubMed: 16019223]
14. Purves RW, Barnett DA, Guevremont R. Separation of protein conformers using electrospray-high field asymmetric waveform ion mobility spectrometry-mass spectrometry. Int J Mass Spectrom. 2000; 197:163–177.
15. Robinson EW, Leib RD, Williams ER. The role of conformation on electron capture dissociation of ubiquitin. J Am Soc Mass Spectrom. 2006; 17:1469–1479. [PubMed: 16890453]
16. Oh H, Breuker K, Sze SK, Ge Y, Carpenter BK, McLafferty FW. Secondary and tertiary structures of gaseous protein ions characterized by electron capture dissociation mass spectrometry and photofragment spectroscopy. Proc Natl Acad Sci U S A. 2002; 99:15863–15868. [PubMed: 12444260]

17. Oh HB, Lin C, Hwang HY, Zhai HL, Breuker K, Zabrouskov V, Carpenter BK, McLafferty FW. Infrared photodissociation spectroscopy of electrosprayed ions in a Fourier transform mass spectrometer. J Am Chem Soc. 2005; 127:4076–4083. [PubMed: 15771545]
18. Valle JJ, Eyler JR, Oomens J, Moore DT, van der Meer AFG, von Helden G, Meijer G, Hendrickson CL, Marshall AG, Blakney GT. Free electron laser-Fourier transform ion cyclotron resonance mass spectrometry facility for obtaining infrared multiphoton dissociation spectra of gaseous ions. Rev Sci Instrum. 2005:76.
19. Oomens J, Polfer N, Moore DT, van der Meer L, Marshall AG, Eyler JR, Meijer G, von Helden G. Charge-state resolved mid-infrared spectroscopy of a gas-phase protein. Physical Chemistry Chemical Physics. 2005; 7:1345–1348. [PubMed: 19787952]
20. Lin C, Infusini G, Oh H, Hwang HY, Breuker K, Kong X, Carpenter BK, McLafferty FW. Infrared Photodissociation Spectroscopy of Gaseous Protein Ions. Techniques and Unusual Hydrogen Bonding. 2007 submitted.
21. Zubarev RA, Kelleher NL, McLafferty FW. Electron capture dissociation of multiply charged protein cations. A nonergodic process. J Am Chem Soc. 1998; 120:3265–3266.
22. Leymarie N, Costello CE, O'Connor PB. Electron capture dissociation initiates a free radical reaction cascade. J Am Chem Soc. 2003; 125:8949–8958. [PubMed: 12862492]
23. Zubarev RA, Horn DM, Fridriksson EK, Kelleher NL, Kruger NA, Lewis MA, Carpenter BK, McLafferty FW. Electron capture dissociation for structural characterization of multiply charged protein cations. Anal Chem. 2000; 72:563–573. [PubMed: 10695143]
24. Horn DM, Breuker K, Frank AJ, McLafferty FW. Kinetic intermediates in the folding of gaseous protein ions characterized by electron capture dissociation mass spectrometry. J Am Chem Soc. 2001; 123:9792–9799. [PubMed: 11583540]
25. Breuker K, Oh HB, Horn DM, Cerda BA, McLafferty FW. Detailed unfolding and folding of gaseous ubiquitin ions characterized by electron capture dissociation. J Am Chem Soc. 2002; 124:6407–6420. [PubMed: 12033872]
26. Breuker K, Oh HB, Lin C, Carpenter BK, McLafferty FW. Nonergodic and conformational control of the electron capture dissociation of protein cations. Proc Natl Acad Sci U S A. 2004; 101:14011–14016. [PubMed: 15381764]
27. Comisarow MB, Marshall AG. Fourier transform ion cyclotron resonance spectroscopy. Chem Phys Lett. 1974; 25:282–283.
28. Marshall AG, Hendrickson CL, Jackson GS. Fourier transform ion cyclotron resonance mass spectrometry: A primer. Mass Spectrom Rev. 1998; 17:1–35. [PubMed: 9768511]
29. Horn DM, Zubarev RA, McLafferty FW. Automated de novo sequencing of proteins by tandem high-resolution mass spectrometry. Proc Natl Acad Sci U S A. 2000; 97:10313–10317. [PubMed: 10984529]
30. Ge Y, Lawhorn BG, ElNaggar M, Strauss E, Park JH, Begley TP, McLafferty FW. Top down characterization of larger proteins (45 kDa) by electron capture dissociation mass spectrometry. J Am Chem Soc. 2002; 124:672–678. [PubMed: 11804498]
31. Zubarev RA. Electron-capture dissociation tandem mass spectrometry. Curr Opin Biotechnol. 2004; 15:12–16. [PubMed: 15102460]
32. Cooper HJ, Hakansson K, Marshall AG. The role of electron capture dissociation in biomolecular analysis. Mass Spectrom Rev. 2005; 24:201–222. [PubMed: 15389856]
33. Savitski MM, Nielsen ML, Kjeldsen F, Zubarev RA. Proteomics-grade de novo sequencing approach. J Proteome Res. 2005; 4:2348–2354. [PubMed: 16335984]
34. Sze SK, Ge Y, Oh H, McLafferty FW. Top-down mass spectrometry of a 29-kDa protein for characterization of any posttranslational modification to within one residue. Proc Natl Acad Sci U S A. 2002; 99:1774–1779. [PubMed: 11842225]
35. Pesavento JJ, Kim YB, Taylor GK, Kelleher NL. Shotgun Annotation of Histone Modifications: A New Approach for Streamlined Characterization of Proteins by Top Down Mass Spectrometry. J Am Chem Soc. 2004; 126:3386–3387. [PubMed: 15025441]
36. Meng F, Forbes AJ, Miller LM, Kelleher NL. Detection and localization of protein modifications by high resolution tandem mass spectrometry. Mass Spectrom Rev. 2005; 24:126–134. [PubMed: 15389861]

37. Savitski MM, Nielsen ML, Zubarev RA. ModifiComb, a new proteomic tool for mapping substoichiometric post-translational modifications, finding novel types of modifications, and fingerprinting complex protein mixtures. Mol Cell Proteomics. 2006; 5:935–948. [PubMed: 16439352]
38. Zhao C, Sethuraman M, Clavreul N, Kaur P, Cohen RA, O'Connor PB. Detailed map of oxidative post-translational modifications of human P21Ras using Fourier transform mass spectrometry. Anal Chem. 2006; 78:5134–5142. [PubMed: 16841939]
39. Patriksson A, Adams C, Kjeldsen F, Raber J, van der Spoel D, Zubarev RA. Prediction of NC[alpha] bond cleavage frequencies in electron capture dissociation of Trp-cage dications by force-field molecular dynamics simulations. Int J Mass Spectrom. 2006; 248:124–135.
40. Tsybin, YO.; He, H.; Hamidane, HB.; Emmett, MR.; Hendrickson, CL.; Tsybin, OY.; Marshall, AG. Electron Capture/Transfer Dissociation Product Ion Abundances: Correlation with Amino Acid Hydrophobicity and Application in Peptide and Protein Structural Analysis. Proceedings of the 54th ASMS Conference on Mass Spectrometry and Allied Topics; Indianapolis, IN. 2007. DVD-ROM
41. Horn DM, Ge Y, McLafferty FW. Activated ion electron capture dissociation for mass spectral sequencing of larger (42 kDa) proteins. Anal Chem. 2000; 72:4778–4784. [PubMed: 11055690]
42. Hakansson K, Chalmers MJ, Quinn JP, McFarland MA, Hendrickson CL, Marshall AG. Combined electron capture and infrared multiphoton dissociation for multistage MS/MS in a Fourier transform ion cyclotron resonance mass spectrometer. Anal Chem. 2003; 75:3256–3262. [PubMed: 12964777]
43. Sze SK, Ge Y, Oh HB, McLafferty FW. Plasma electron capture characterization of large dissociation for the proteins by top down mass spectrometry. Anal Chem. 2003; 75:1599–1603. [PubMed: 12705591]
44. Tsybin YO, Witt M, Baykut G, Kjeldsen F, Hakansson P. Combined infrared multiphoton dissociation and electron capture dissociation with a hollow electron beam in Fourier transform ion cyclotron resonance mass spectrometry. Rapid Commun Mass Spectrom. 2003; 17:1759–1768. [PubMed: 12872281]
45. Oh HB, McLafferty FW. A variety of activation methods employed in "activated-ion" electron capture dissociation mass spectrometry: A test against bovine ubiquitin 7+ions. Bull Korean Chem Soc. 2006; 27:389–394.
46. Cournoyer, JC.; Lin, C.; O'Connor, PB. Using H(dot) Transfer from Electron Capture Dissociation Fragmentation Spectra to Probe the Gas-Phase Structure of Peptides. 2007. Submitted
47. Gauthier JW, Trautman TR, Jacobson DB. Sustained Off-Resonance Irradiation for Collision-Activated Dissociation Involving Fourier-Transform Mass-Spectrometry - Collision-Activated Dissociation Technique That Emulates Infrared Multiphoton Dissociation. Anal Chim Acta. 1991; 246:211–225.
48. Mirgorodskaya E, O'Connor PB, Costello CE. A general method for precalculation of parameters for sustained off resonance irradiation/collision-induced dissociation. J Am Soc Mass Spectrom. 2002; 13:318–324. [PubMed: 11951969]
49. Dunbar RC, McMahon TB. Activation of Unimolecular Reactions by Ambient Blackbody Radiation. Science. 1998; 279:194–197.
50. Price WD, Schnier PD, Williams ER. Tandem mass spectrometry of large biomolecule ions by blackbody infrared radiative dissociation. Anal Chem. 1996; 68:859–866. [PubMed: 21619182]
51. O'Connor PB, Lin C, Cournoyer JJ, Pittman JL, Belyayev M, Budnik BA. Long-Lived Electron Capture Dissociation Product Ions Experience Radical Migration via Hydrogen Abstraction. J Am Soc Mass Spectrom. 2006; 17:576–585. [PubMed: 16503151]
52. Savitski MM, Kjeldsen F, Nielsen ML, Zubarev RA. Hydrogen rearrangement to and from radical z fragments in electron capture dissociation of peptides. J Am Soc Mass Spectrom. 2007; 18:113–120. [PubMed: 17059886]
53. Tsybin YO, He H, Emmett MR, Hendrickson CL, Marshall AG. Ion Activation in Electron Capture Dissociation to Distinguish Between N-terminal and C-terminal Product Ions. Anal Chem. 2007; 79:7596–7602. [PubMed: 17874851]

54. Lin C, O'Connor PB, Cournoyer JJ. Use of a double resonance electron capture dissociation experiment to probe fragment intermediate lifetimes. J Am Soc Mass Spectrom. 2006; 17:1605–1615. [PubMed: 16904337]
55. O'Connor PB, Pittman JL, Thomson BA, Budnik BA, Cournoyer JC, Jebanathirajah J, Lin C, Moyer S, Zhao C. A new hybrid electrospray Fourier transform mass spectrometer: design and performance characteristics. Rapid Commun Mass Spectrom. 2006; 20:259–266. [PubMed: 16353130]
56. Jebanathirajah JA, Pittman JL, Thomson BA, Budnik BA, Kaur P, Rape M, Kirschner M, Costello CE, O'Connor PB. Characterization of a new qQq-FTICR mass spectrometer for post-translational modification analysis and top-down tandem mass Spectrometry of whole proteins. J Am Soc Mass Spectrom. 2005; 16:1985–1999. [PubMed: 16271296]
57. Mihalca R, Kleinnijenhuis AJ, McDonnell LA, Heck AJR, Heeren RMA. Electron capture dissociation at low temperatures reveals selective dissociations. J Am Soc Mass Spectrom. 2004; 15:1869–1873. [PubMed: 15589763]
58. Gill AC, Jennings KR, Wyttenbach T, Bowers MT. Conformations of biopolymers in the gas phase: a new mass spectrometric method. Int J Mass Spectrom. 2000; 196:685–697.
59. Liu HC, Hakansson K. Divalent metal ion-peptide interactions probed by electron capture dissociation of trications. J Am Soc Mass Spectrom. 2006; 17:1731–1741. [PubMed: 16952459]
60. Cooper HJ, Hudgins RR, Hakansson K, Marshall AG. Secondary fragmentation of linear peptides in electron capture dissociation. Int J Mass Spectrom. 2003; 228:723–728.
61. Zubarev RA. Reactions of polypeptide ions with electrons in the gas phase. Mass Spectrom Rev. 2003; 22:57–77. [PubMed: 12768604]
62. Turecek F. N-C-alpha bond dissociation energies and kinetics in amide and peptide radicals. Is the dissociation a non-ergodic process? J Am Chem Soc. 2003; 125:5954–5963. [PubMed: 12733936]
63. Yao CX, Syrstad EA, Turecek F. Electron transfer to protonated beta-alanine N-methylamide in the gas phase: An experimental and computational study of dissociation energetics and mechanisms. Journal of Physical Chemistry A. 2007; 111:4167–4180.
64. Kjeldsen F, Haselmann KF, Budnik BA, Jensen F, Zubarev RA. Dissociative capture of hot (3–13 eV) electrons by polypeptide polycations: an efficient process accompanied by secondary fragmentation. Chem Phys Lett. 2002; 356:201–206.
65. Kjeldsen F, Zubarev R. Secondary losses via gamma-lactam formation in hot electron capture dissociation: A missing link to complete de novo sequencing of proteins? J Am Chem Soc. 2003; 125:6628–6629. [PubMed: 12769561]
66. Belyayev MA, Cournoyer JJ, Lin C, O'Connor PB. The effect of radical trap moieties on electron capture dissociation spectra of Substance P. J Am Soc Mass Spectrom. 2006; 17:1428–1436. [PubMed: 16875835]
67. Hayakawa S, Hashimoto M, Matsubara H, Turecek F. Dissecting the proline effect: Dissociations of proline radicals formed by electron transfer to protonated pro-gly and gly-pro dipeptides in the gas phase. J Am Chem Soc. 2007; 129:7936–7949. [PubMed: 17550253]
68. Jones JW, Sasaki T, Goodlett DR, Turecek F. Electron capture in spin-trap capped peptides. An experimental example of ergodic dissociation in peptide cation-radicals. J Am Soc Mass Spectrom. 2007; 18:432–444. [PubMed: 17112737]

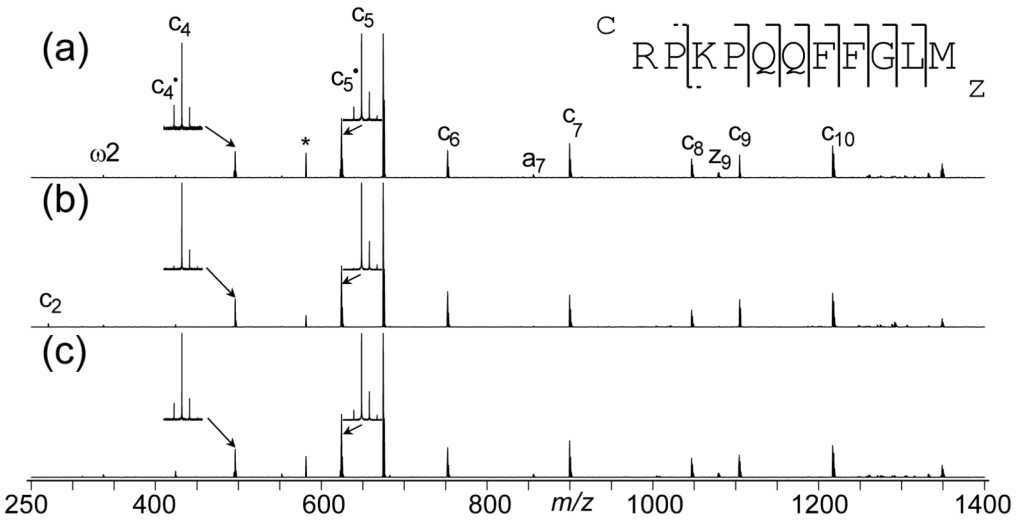

Figure 1.
ECD spectra of substance P with 150 ms electron irradiation and (a) no IR irradiation; (b) 200 ms IR irradiation immediately before the ECD event; and (c) 200 ms IR irradiation immediately after the ECD event. * marks electronic noise.

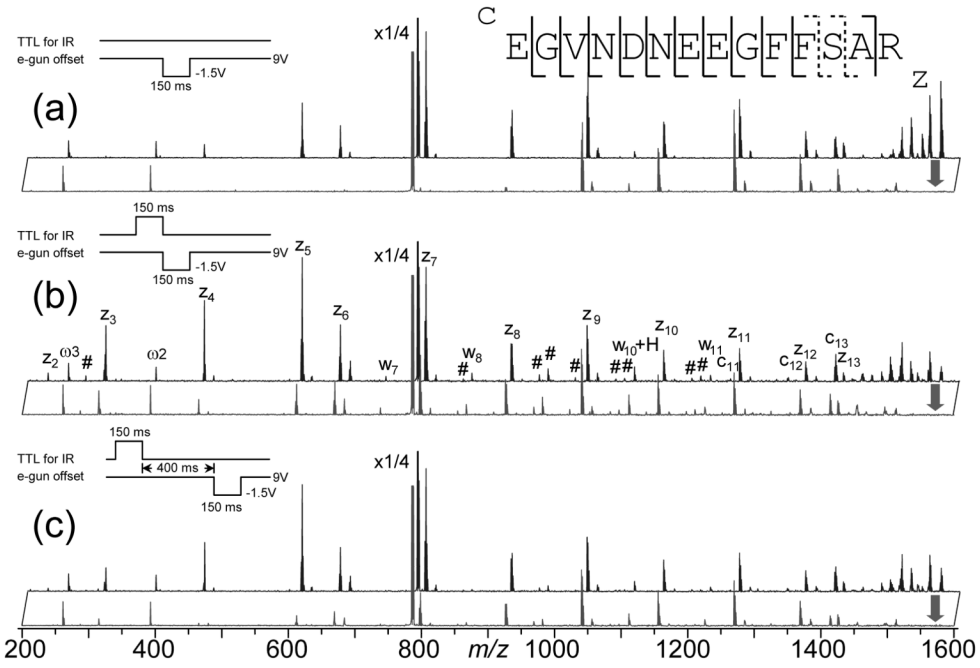

Figure 2.

ECD (upper) and DR-ECD (lower) spectra of fibrinopeptide B with 150 ms electron irradiation and (a) no IR irradiation; (b) 150 ms IR irradiation immediately before the ECD event; and (c) 150 ms IR irradiation, followed by a 400 ms delay, before the ECD event. Insets illustrate the pulse sequence used in each experiment. For clarity, only c, z and w type ions are labeled, and # indicates secondary fragments corresponding to additional side chain losses from z-type ions. Dashed cleavages are observed in AI-ECD only.

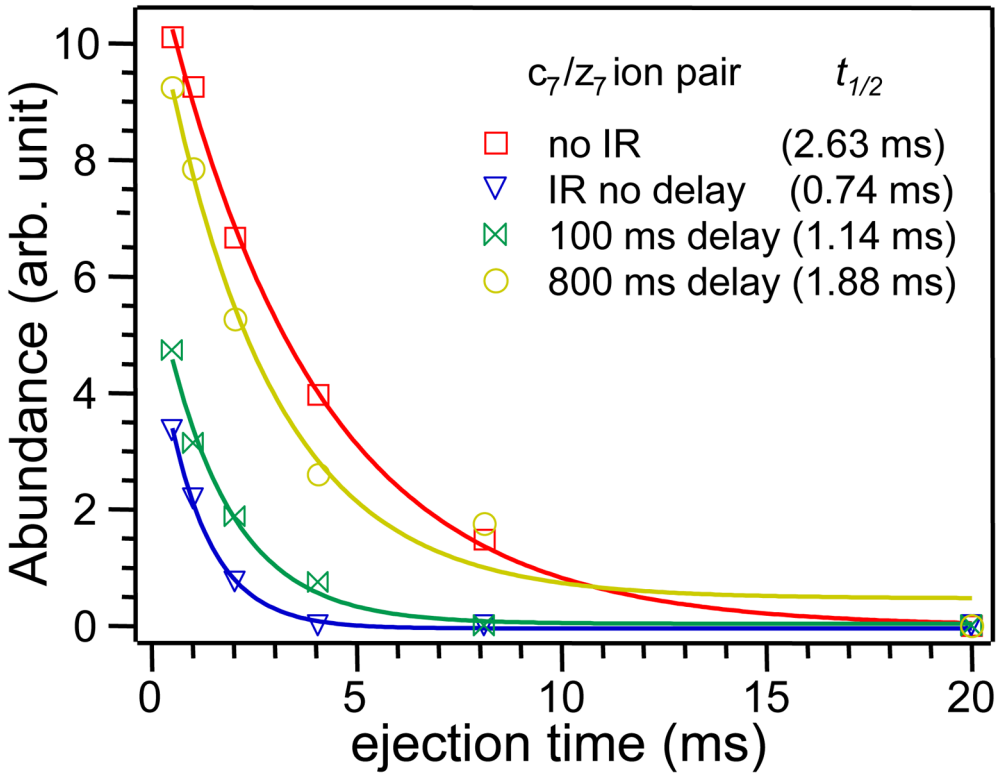

Figure 3.
First order decays of the intact c_7/z_7 ion pair abundance as a function of ejection time when ECD of fibrinopeptide B was carried out at various delays after the IR irradiation. Solid lines are single exponential fits.

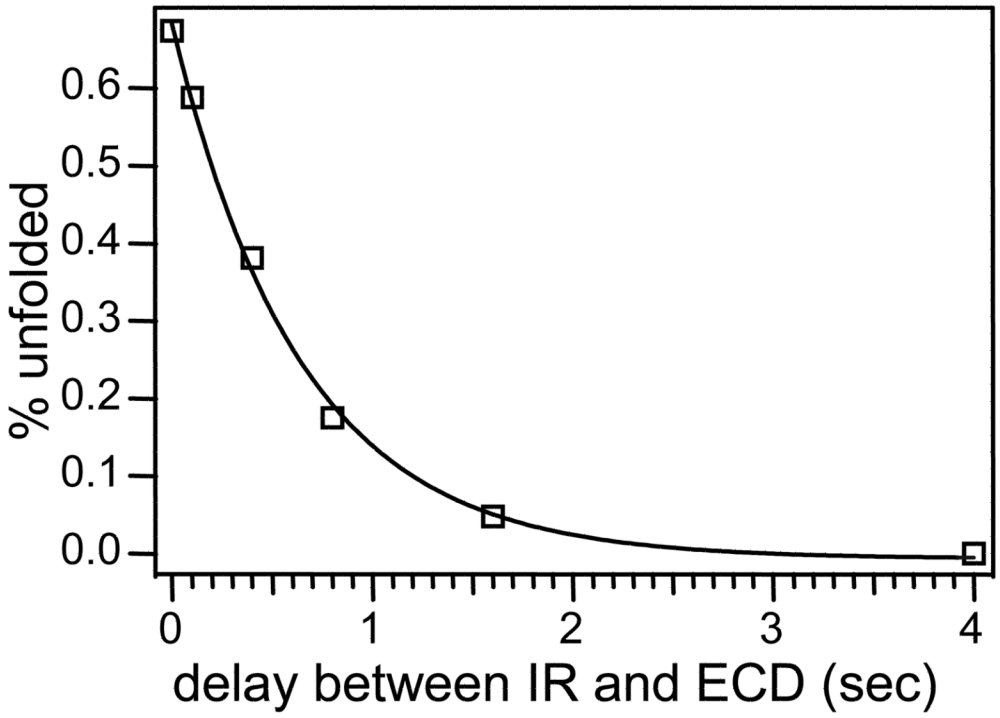

Figure 4.
Percentage of the fibrinopeptide B ions that remained unfolded (as calculated from the DR-ECD experiment) at various time delays after the IR irradiation was turned off. Solid line is the single exponential fit.

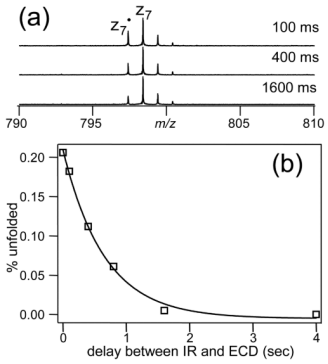

Figure 5.

(a) Expanded regions of the ECD spectra of fibrinopeptide B showing that the percentage of the hydrogen transfer product (z_7) increased as the delay between the IR and ECD events increased. (b) Percentage of the fibrinopeptide B ions that remained unfolded (as calculated from the ratio of $z_7^{\bullet}$ and z_7 abundances) at various time delays after the IR irradiation was turned off. Solid line is the single exponential fit.

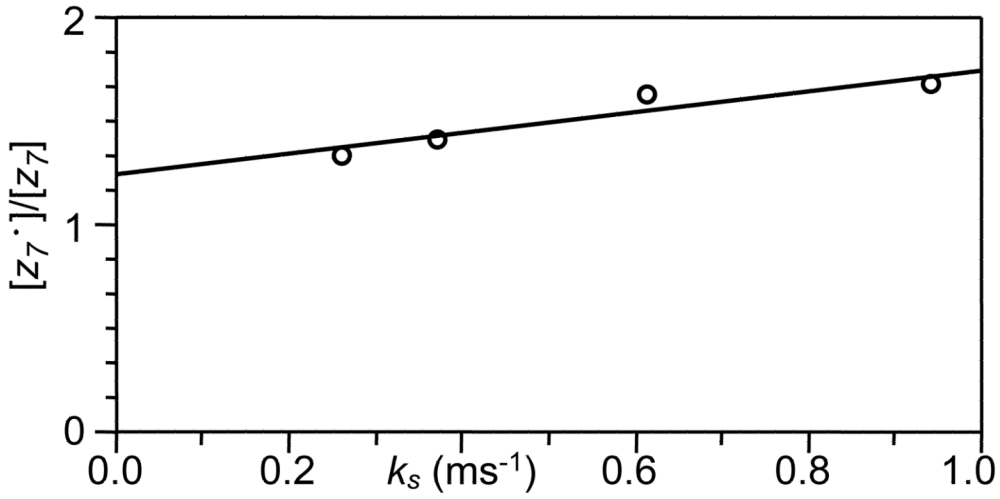

Figure 6.
Linear fit of the ratio of the $z_7^{\bullet}$ and z_7 abundances as a function of the ion separation rate constant as calculated from the DR-ECD experiments.